Two-State On-Off Intermittency and the Onset of Turbulence in a Spatiotemporally Chaotic System

P. P. Galuzio, S. R. Lopes, and R. L. Viana
Departamento de Física, Universidade Federal do Paraná, 81531-990, Curitiba, PR, Brazil
(Received 4 March 2010; published 27 July 2010)

We show the existence of two-state on-off intermittent behavior in spatially extended dynamical systems, using as an example the damped and forced drift wave equation. The two states are stationary solutions corresponding to different wave energies. In the language of (Fourier-mode) phase space these states are embedded in two invariant manifolds that become transversely unstable in the regime where two-state on-off intermittency sets in. The distribution of laminar duration sizes is compatible with the similar phenomenon occurring in time only in the presence of noise. In an extended system the noisy effect is provided by the spatial modes excited by the perturbation. We show that this intermittency is a precursor of the onset of strong turbulence in the system.

DOI: 10.1103/PhysRevLett.105.055001 PACS numbers: 52.35.Mw, 05.45.Jn

The onset of turbulence in spatiotemporal systems is a long-standing problem of paramount importance, which has been studied intensively [1]. If we consider a Fourier-mode description of the transition to turbulence in a spatially extended dynamical system, the onset of turbulence occurs when the system energy, originally concentrated in the temporal degree of freedom, is distributed among the spatial modes. Moreover, the temporal dynamics must present a chaotic attractor acting as a stochastic pump, by feeding energy to the spatial modes to be excited in order to yield irregular spatial behavior [2,3]. In a previous paper, we described this process in a system of three waves nonlinearly coupled through interactions of a wave triplet subjected to a resonance condition [4]. The temporal dynamics, exhibiting chaotic behavior but a periodic spatial profile, can be viewed geometrically as a low-dimensional manifold embedded in the phase space consisting of the Fourier modes retained in the procedure to solve the system. The onset of turbulence occurs when this manifold loses transversal stability and trajectories explore more spatial degrees of freedom, imparting energy to the corresponding spatial modes [5].

In this Letter we consider a situation where there are two manifolds instead of only one, in each of which lie stationary solutions of a periodically forced nonlinear wave equation corresponding to different wave energies. These manifolds lose transversal stability through the same process as before, but there are novel features in this case. The most important is that both manifolds may be transversely unstable. In this case the trajectories wander through the available phase space volume approaching the vicinity of both manifolds in an erratic way. This behavior, also known as two-state on-off intermittency, has been described in low-dimensional dynamical systems [6] as well as in spatially extended systems [7]. In this kind of intermittency there is an alternating behavior between two different stationary states. Because of the chaotic behavior in each state, these alternations occur for different and irregularly spaced time intervals. Two-state intermittency differs from on-off intermittency [8] because the system state, after departing from a given state, goes to the vicinity of another state, the transient behavior between them being governed by a chaotic saddle [9]. In spatially extended systems the dynamics at either state lies on a manifold embedded in the phase space.

As a representative example of a spatially extended dynamical system with two solution branches, we consider the damped and forced drift wave equation [10,11]

$$\phi_t + a\phi_{txx} + c\phi_x + f\phi\phi_x + \gamma\phi = -\epsilon \sin(Kx - \Omega t). \tag{1}$$

For magnetically confined fusion plasmas $\phi(x, t)$ is the nondimensional electric potential of a drift wave propagating along the poloidal direction of a toroidal plasma, where the constants a, c, and f stand for plasma and wave parameters, and we introduced a linear damping term with coefficient γ [12]. The effect of other possibly relevant modes is represented by a time-periodic driving with amplitude ϵ, wave number K, and frequency Ω, representing the inductor wave.

Equation (1), for certain parameter values, displays a transition from pure temporal chaos without spatial mode excitation to spatiotemporal chaos. We found that the solutions wander in an intermittent fashion between two nonoverlapping states of distinct wave energies, hence an example of two-state on-off intermittency in a higher-dimensional system of physical interest. In previous works [10,13,14] such a transition was also reported to be due to an interior crisis, resulting from a collision between a chaotic attractor and an unstable periodic orbit. We believe that both scenarios can arise due to different initial conditions, since this high-dimensional dynamical system must possess an involved basin of attraction structure, with many coexisting different scenarios.

Provided the x- coordinate is a bounded variable, we suppose a Fourier expansion $\phi(x,t) = \sum_{n=0}^{N} \varphi_n(t) \times \exp(i\kappa_n x)$, where $\varphi_n(t)$ are time-dependent amplitudes and $\kappa_n \equiv 2\pi n/L$ in a box of length $L = 2\pi$ and periodic boundary conditions. Notice that the mode $\kappa_0 = 0$ is purely temporal, whereas $\kappa_\alpha = \alpha = 1, 2, 3, \ldots$ stand for the spatial modes. One obtains a system of N coupled ordinary differential equations, solved using a predictor-corrector scheme. In the numerical simulations we used $N = 128$ modes, unless stated otherwise, and we kept fixed the following parameters [12]: $a = -0.287\,11$, $c = 1.0$, $f = -6.0$, $\gamma = 0.1$, $K = 1.0$, and $\Omega = 0.65$, such that ϵ will be our control parameter. The initial conditions for the system of N coupled mode equations are $\varphi(0) = 0.01$, $\varphi_1(0) = \varphi_2(0) = \sigma_1 R(0,1)$, $\varphi_n(0) = \sigma_2 R(0,1)$, for $n \geq 3$, where $\sigma_1 = 0.001$, $\sigma_2 = 10^{-5}$, and $R(0,1)$ is a pseudorandom number chosen within the interval $[0,1]$ with uniform probability. We stress that these initial conditions are different from those used in Ref. [12], where a solitary-wave solution of the unperturbed case ($\epsilon = 0$, $\gamma = 0$) was chosen.

The solutions of the initial and boundary value problem defined by Eq. (1) can be characterized by the wave energy, defined as

$$E(t) = \frac{1}{2\pi} \int_0^{2\pi} \frac{1}{2} [\phi^2(x,t) - a\phi_x^2(x,t)] dx, \qquad (2)$$

which turns out to be an integral of motion for the unperturbed case. Since E is a scalar measure, its time evolution cannot be thought to be a projection of some higher-dimensional variable of the system. For the parameter values explored in this work the wave dynamics is chaotic, but even so the energy difference is bounded [13,14].

In Fig. 1 we exhibit the time evolution of the energy difference $\Delta E = E(t) - E(0)$ for selected values of the control parameter ϵ. As the latter is increased from zero, we have a steady state energy with a few peaks, and asymptoting to a value of about 0.05 [Fig. 1(a)], until a first bifurcation value $\epsilon_\ell = 0.199\,55$ is achieved. For $\epsilon_\ell < \epsilon < \epsilon_h = 0.201\,00$, we have alternation of energy values between two values, the former $\sim$0.05 lower branch and a $\sim$0.25 higher branch [Fig. 1(b)]. Finally, for $\epsilon > \epsilon_h$ the energy fluctuates about the higher branch value, never to return to the lower branch [Fig. 1(c)]. Our main point in this Letter is that the lower and upper branches of the wave energy are two energy states for which, when $\epsilon_\ell < \epsilon < \epsilon_h$, there is intermittent behavior. These two states can be represented, in the Fourier-mode space, by different energy hypersurfaces we call A and B. For $\epsilon < \epsilon_\ell$ the state A is stable with respect to transversal displacements from the energy hypersurface, whereas B is transversely unstable and not reached by typical initial conditions [Fig. 1(a)].

Figure 1(d) shows a scheme of the situation, in which the states A and B have average energies of 0.05 and 0.25, respectively. The shaded regions represent the maximum fluctuations of the energy about these states, in order to emphasize that there is no overlapping between them. The state A loses transversal stability at $\epsilon = \epsilon_\ell$ and B becomes transversely stable at $\epsilon = \epsilon_h$. The existence of these two bifurcation points has long been known and has been related to hysteretical behavior when increasing and/or decreasing ϵ through these critical values [12]. For the set of initial conditions used here, however, since the energy excursions are bounded and nonoverlapping, there cannot be such hysteretical behavior, since none of these states are transversely stable. Another observable consequence of the transversal stability properties of the states A and B is that, for $\epsilon_\ell < \epsilon < \epsilon_h$, both manifolds are transversely unstable, and the wave energy makes intermittent transitions between these two states [Fig. 1(b)]. Finally, for $\epsilon > \epsilon_h$ only the state B is transversely stable and two-state intermittency ceases [as in Fig. 1(c)].

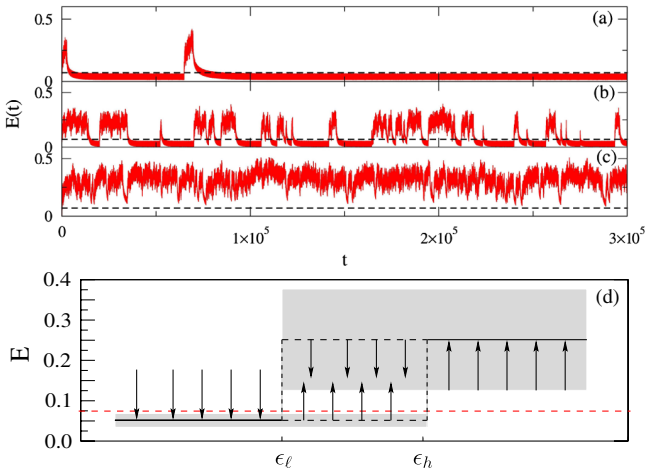

FIG. 1 (color online). Time evolution of the energy difference for (a) $\epsilon = 0.199\,553 \lesssim \epsilon_\ell$, (b) $\epsilon_\ell < \epsilon = 0.200\,25 < \epsilon_h$, (c) $\epsilon = 0.201\,75 \gtrsim \epsilon_h$. The dashed line is the limit of bounded variation for the fluctuations of the lower energy state. (d) Schematic figure showing the two energy states and their corresponding transversal stability. The shaded regions represent the intervals of bounded variation of energy fluctuations about their average values (shown as solid lines and dashed lines for transversely stable and unstable cases, respectively).

Since a few temporal modes are excited in the state A, it corresponds to temporal chaos combined with regular spatial patterns. This is illustrated by the space-time plot depicted in Fig. 2(a), obtained for $\epsilon < \epsilon_\ell$, which displays a chaotic time evolution with regular spatial behavior akin to a traveling wave solution. However, as the state B becomes transversely stable, a large number of spatial modes are excited. An extreme example, considering $\epsilon > \epsilon_h$, is shown in Fig. 2(b), for which we see aperiodic behavior in both spatial and temporal scales (spatiotemporal chaos). For a small interval of time (*circa* 25 pseudo-periods), some traveling waves, which appear due to the inductor term, are continuously created and destroyed.

In order to provide a quantitative characterization of the dynamics in space and time, we can resort to Lyapunov

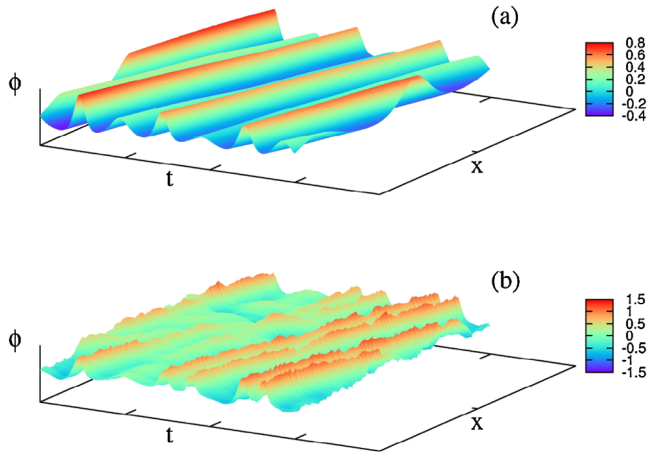

FIG. 2 (color online). Space-time plots for the wave amplitude for (a) $\epsilon = 0.1990 < \epsilon_\ell$ and (b) $\epsilon = 0.2100 > \epsilon_h$.

exponent computation in Fourier space. In this case, each Fourier mode in the discrete transform can be considered a degree of freedom, and the corresponding Lyapunov exponent is computed from the set of N ordinary differential equations for the wave amplitudes $\varphi_n(t)$, with $n = 0, 1, 2, \ldots, N$. The exponent related to $n = 0$ corresponds to the temporal dynamics, whereas the $n \geq 1$ case stands for spatial degrees of freedom and can be used to detect spatial mode excitation [4].

Accordingly, in Fig. 3 we plot the time evolution of the 30 first Lyapunov exponents out of $N = 128$. The symbols λ_L and λ_T stand for longitudinal and transversal exponents, respectively. We assume the Lyapunov exponents to be zero if their average decay is a power law and negative if they decay faster than a power law. In the case of $\epsilon = 0.195 < \epsilon_\ell$, only the Lyapunov exponent related to the time ($n = 0$) asymptotes to a nonzero value [Fig. 3(a)], confirming our claim that only temporal chaos is observed. The exponents corresponding to spatial modes are shown

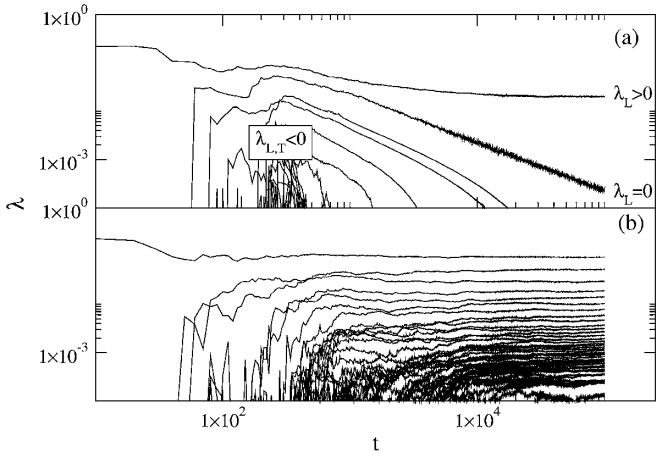

FIG. 3. The 30 largest Lyapunov exponents corresponding to modes in Fourier space for (a) $\epsilon = 0.195$ and (b) $\epsilon = 0.205$.

to decay in a roughly power law ($n = 1$) and even faster rates (for $n \geq 2$). Hence those spatial modes, if excited at all, can have at most periodic behavior (and a possible quasiperiodic one). By way of contrast, for $\epsilon > \epsilon_h$ a large number of the exponents for $n \neq 0$ do not vanish, hence many spatial modes become chaotic [Fig. 3(b)]. This spatial mode excitation involving so many Fourier modes suggests the existence of a strongly turbulent state.

The existence of strong turbulence can actually be tested by computing the Fourier spectrum of the waves $|\bar{\varphi}(\kappa_n)| = (1/t_{\max}) \sum_{t=0}^{t_{\max}} |\varphi_n(t)|$, where $\kappa_n = n$. When there is temporal chaos only [i.e., for $\epsilon < \epsilon_\ell$, cf. Fig. 4(a)], we have an energy spectrum that decays faster than a power law, starting from a maximum value at $\kappa_n = 3$. A least-squares fit gives an exponential scaling $|\bar{\varphi}(\kappa_n)| \sim e^{-\sigma \kappa_n}$, with $\sigma = 0.737 \pm 0.014$. However, in the upper energy branch B, where we believe that a strong turbulent state sets in, the computed Fourier spectrum can be fitted by a power law of the form $|\bar{\varphi}(\kappa_n)| \sim \kappa_n^{-\varpi}$, where $\varpi = 1.558 \pm 0.019$ [Fig. 4(b)]. In Fig. 4(b) we have used $N = 1024$ modes. It has been necessary to increase the number of modes in this case since, in such a fully turbulent scenario, there is a strong interaction among different spatial scales, leading to a fast redistribution of the wave energy to the lowest wavelengths.

Our numerical evidences of strong turbulent behavior in the upper energy branch B are based on the Taylor hypothesis; namely, we can relate the spatial statistics corresponding to a fixed time to the statistics of a time series measured at a *single* point of space [15]. Hence we may characterize the turbulent behavior by the energy spectrum as a function of the frequency rather than the wave number. The energy spectrum $E(\nu)$ corresponding to the Fourier spectra we considered above is depicted in Fig. 4(c), where

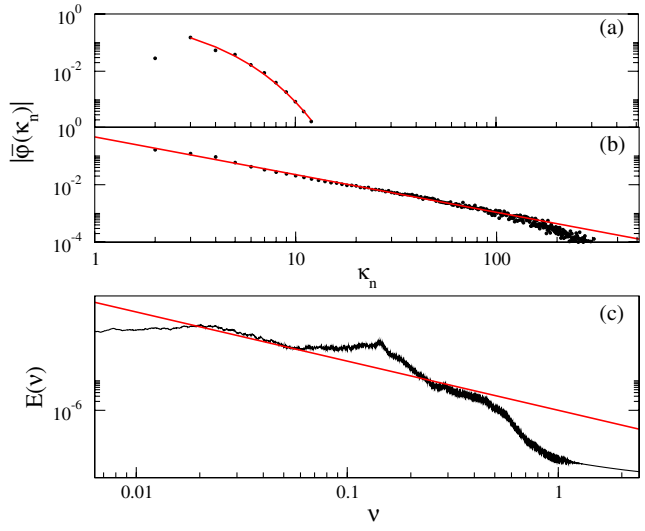

FIG. 4 (color online). Fourier spectra for (a) $\epsilon = 0.1990$ and (b) $\epsilon = 0.2100$. (c) Wave energy spectrum for $\epsilon = 0.2100$. The solid line is the Kolmogorov 5/3 scaling law.

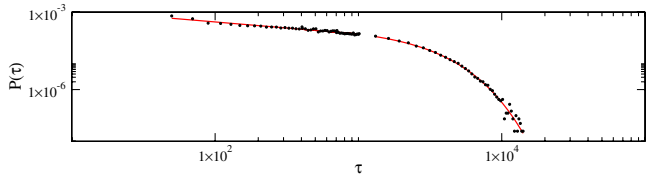

FIG. 5 (color online). Histogram showing the distribution of the plateau sizes for the laminar region A and $\epsilon = 0.200\,75$.

we superimposed a straight line corresponding to the Kolmogorov scaling $E(\nu) \sim \nu^{-5/3}$ to guide the eye. We see three frequency intervals with respect to the Kolmogorov scaling: (i) for small frequencies we have the familiar $1/f$-noise behavior; (ii) an interval $0.02 \gtrsim \nu \gtrsim 0.5$ which obeys the $5/3$ scaling except for a peak near 0.1, which is related to the inductor wave with frequency $\Omega/2\pi \approx 0.1034$; (iii) for large frequencies the scaling is exponential (heavy tail).

Two-state on-off intermittency occurs in the case $\epsilon_\ell < \epsilon < \epsilon_h$ and is characterized by the irregular alternations between the two energy branches A and B, which are transversely unstable in the Fourier-mode phase space of the system. If the trajectory starts at a point close (off but very near) to A, the system stays for some time at the lower energy branch, until it approaches a transversely unstable periodic orbit embedded in the invariant manifold A and is ejected away from A towards B, essentially the same behavior occurring there. By adopting a small tolerance in the vicinity of each invariant manifold, we can define ''laminar'' states—or plateaus—as those in which the dynamics is very near either of the invariant manifolds. The duration of these plateaus is rather arbitrary since the dynamics is temporally chaotic and the system ergodically approaches every accessible transversely unstable orbit in both manifolds. Hence, a statistical characterization of the two-state on-off intermittency can be given by the probability distribution function of the plateau sizes (or laminar durations) τ_i in the intermittent regime. A numerical approximation of this probability distribution function is provided in Fig. 5, where we plot a histogram of the plateau sizes. We have two scaling regimes: (i) a power law $P(\tau) \sim \tau^{-\beta}$, with $\beta = -0.469 \pm 0.016$, valid for small plateaus, and (ii) an exponential (or heavy) tail $P(\tau) \sim e^{\gamma\tau}$, with $\gamma = -0.000\,67 \pm 0.000\,01$ for large plateaus. The existence of these two scalings is a characteristic feature of on-off intermittency with noise, the existent crossover between them being related to the noise level. In a spatially extended system the noisy effect is provided by the irregular forcing of the spatial modes excited in the Fourier space.

In summary, we proposed a new scenario for the onset of intermittent behavior in complex systems having two nonoverlapping and bounded energy states. The underlying mechanism of the transition is an extension of the two-state on-off intermittency to spatially extended systems, and it is complementary to other scenarios whereby this transition may occur via a crisis. The basic difference between these scenarios is that, in the latter one, the energy states present overlapping excursions. Both scenarios may appear as a result of different initial conditions since the basin structure of spatially extended systems is highly involved. Our results can be a theoretical basis for explaining intermittent structures in turbulent signals from fusion plasma experiments [16].

This work has partial financial support of CNPq, CAPES, Fundação Araucária, and RNF-CNEN (Brazilian Fusion Network).

[1] U. Frisch, *Turbulence: The Legacy of A. N. Kolmogorov* (Cambridge University Press, Cambridge, England, 1995).
[2] G. Corso and A. J. Lichtenberg, Phys. Rev. E **59**, 6652 (1999).
[3] S. R. Lopes and F. B. Rizzato, Phys. Rev. E **60**, 5375 (1999).
[4] J. D. Szezech, Jr., S. R. Lopes, and R. L. Viana, Phys. Rev. E **75**, 067202 (2007).
[5] J. D. Szezech, Jr., S. R. Lopes, R. L. Viana, and I. L. Caldas, Physica (Amsterdam) **238D**, 516 (2009).
[6] Y. Lai and C. Grebogi, Phys. Rev. E **52**, R3313 (1995).
[7] E. Covas, P. Ashwin, and R. Tavakol, Phys. Rev. E **56**, 6451 (1997).
[8] J. F. Heagy, N. Platt, and S. M. Hammel, Phys. Rev. E **49**, 1140 (1994).
[9] E. L. Rempel, A. C.-L. Chian, E. E. N. Macau, and R. Rosa, Chaos **14**, 545 (2004).
[10] E. L. Rempel and A. C.-L. Chian, Phys. Rev. Lett. **98**, 014101 (2007).
[11] W. Horton, Phys. Rep. **192**, 1 (1990).
[12] K. He and A. Salat, Plasma Phys. Controlled Fusion **31**, 123 (1989).
[13] K. He, Phys. Rev. Lett. **94**, 034101 (2005).
[14] K. He and A. C.-L. Chian, Phys. Rev. Lett. **91**, 034102 (2003).
[15] E. Gledzer, Physica (Amsterdam) **104D**, 163 (1997).
[16] V. Antoni, V. Carbone, E. Martines, G. Regnoli, G. Serianni, N. Vianello, and P. Veltri, Europhys. Lett. **54**, 51 (2001).